Natural Rubber Composites Reinforced with Sisal/Oil Palm Hybrid Fibers: Tensile and Cure Characteristics

Maya Jacob,[1] Sabu Thomas,[1] K. T. Varughese[2]

[1]*School of Chemical Sciences, Mahatma Gandhi University, Priyadarshini Hills P.O., Kottayam 686 560, Kerala, India*
[2]*Thermal Research Center, KORADI, Nagpur 441 111, India*

Received 17 March 2003; accepted 5 March 2004
DOI 10.1002/app.20696
Published online in Wiley InterScience (www.interscience.wiley.com).

ABSTRACT: Natural rubber was reinforced with untreated sisal and oil palm fibers chopped to different fiber lengths. The influence of fiber length on the mechanical properties of the hybrid composites was determined. Increasing the fiber length resulted in a decrease in the properties. The effects of concentration on the rubber composites reinforced with sisal/oil palm hybrid fibers were studied. Increasing the concentration of fibers resulted in a reduction in the tensile strength properties and tear strength but an increase in the modulus of the composites. Fiber breakage analysis was evaluated. The vulcanization parameters, processability characteristics, and stress–strain properties of these composites were analyzed. The extent of fiber alignment and the strength of the fiber–rubber interface adhesion were analyzed from the anisotropic swelling measurements. Scanning electron microscopy studies were performed to analyze the fiber/matrix interactions. © 2004 Wiley Periodicals, Inc. J Appl Polym Sci 93: 2305–2312, 2004

Key words: fibers; composites; mechanical properties

INTRODUCTION

Fiber-reinforced rubber composites are of tremendous importance both in end-use applications and in the areas of research and development. These composites exhibit the combined behavior of the soft, elastic rubber matrix and the stiff, strong fibrous reinforcement. The development of fiber-reinforced rubber composites has made available polymers that are harder than aluminum and stiffer than steel. Generally, short-fiber-reinforced rubber composites have become popular in industrial fields because of their processing advantages and increases in strength, stiffness, modulus, and damping.[1,2] The design of a short-fiber-reinforced rubber composite depends on several factors, including the aspect ratio of the fiber, control of the fiber orientation, and dispersion and existence of a strong interface between the fiber and rubber.

Cellulosic fibers are derived from many renewable resources and have many desirable properties for the reinforcement of thermoplastics, including low density, high stiffness, and low cost.[3–8] Various natural fibers have been used as reinforcements in natural rubber (NR); namely, the use of sisal and coir fibers as reinforcing fillers for NR was investigated by Varghese et al.[9] and Geethamma et al.[10] The use of waste silk fiber and jute fiber in NR has also been studied.[11,12] Sisal fiber is one of the strongest fibers and can be used for several applications.[13] Oil palm empty fruit bunch fibers and oil palm mesocarp fibers are two important types of fibrous materials left in the palm oil mill. Because these waste materials create great environmental problems, the economic utilization of these fibers as reinforcements would be beneficial. Oil palm fibers are hard and tough and have been found to be a potential reinforcement in phenol–formaldehyde resins.[14]

Sisal and oil palm fibers appear to be promising materials because of the high tensile strength of sisal fiber and the toughness of oil palm fiber. Therefore, any composite comprised of these two fibers will exhibit the desirable properties of the individual constituents. The properties of a hybrid composite mainly depend on the fiber content, length of individual fibers, orientation, extent of intermingling of fibers, fiber-to-matrix bonding, and arrangement of both of the fibers. The strength of the hybrid composite is also dependent on the failure strain of the individual fibers. This study dealt with the optimization of sisal and oil palm fiber lengths in NR composites. The influence of fiber length and fiber loading on the mechanical properties was analyzed. The extent of fiber alignment and the strength of the fiber–rubber interface adhesion was analyzed from anisotropic swelling measurements.

Correspondence to: S. Thomas (sabut@sancharnet.in).

TABLE I
Properties of Sisal and Oil Palm Fibers

Property	Sisal fiber	Oil palm fiber
Chemical constituents (%)		
Cellulose	78	65
Hemicellulose	10	—
Lignin	8	19
Wax	2	—
Ash	1	2
Physical properties		
Diameter	0.1212 mm	150–500 μm
Density	1.45 g/cm^3	0.7–1.55 g/cc
Tensile strength (MPa)	530–630	248
Young's modulus	17–22 GPa	6700 MPa
Microfibrillar angle (°)	20–25	46
Elongation at break (%)	3–7	14

EXPERIMENTAL

Sisal fiber was obtained from Sheeba Fibers (Poovancode, Tamil Nadu, India). Oil palm fiber was obtained from Oil Palm India, Ltd. (Kottayam, Kerala, India). The NR used for the study was procured from the Rubber Research Institute of India (Kottayam). All of the other ingredients, including zinc oxide, stearic acid, 2,2,4-trimethyl-1,2-dihydroquinoline (TDQ), *N*-cyclohexylbenzothiazyl sulfenamide (CBS), and sulfur, were commercial grade and were obtained from local rubber chemical suppliers.

Fiber preparation

The chemical constituents and physical properties of the fibers are given in Table I. Sisal and oil palm fibers were first separated from undesirable foreign matter and pith material. The fibers were then repeatedly washed with water and were air-dried. The fibers were then chopped to different lengths.

Preparation of the composites

The formulations of the mixes are shown in Table II. NR was masticated on the mill for 2 min followed by the addition of the ingredients. The composite materials were prepared in a laboratory two-roll mill (150 $\times$ 300 mm). The nip gap, mill roll, speed ratio, and number of passes were kept the same for all of the mixes. The samples were milled for sufficient times to disperse the fibers in the matrix at a mill opening of 1.25 mm. The fibers were added at the end of the mixing process, with care taken to maintain the direction of compound flow so that the majority of fibers followed the direction of the flow.

Property measurement

We carried out the fiber breakage analysis by dissolving 1 g of the uncured composite in toluene, followed by the separation of fibers from the solution. The distribution of fiber length was determined with a traveling microscope.

Curing properties were measured in a Monsanto R-100 rheometer at a temperature of 150°C.

Stress–strain measurements were carried out at a crosshead speed of 500 mm/min. Tensile strength and tear strength was measured according to ASTM methods D 412-68 and D 624-54, respectively. The tensile tests were done with dumbbell samples cut at different angles with respect to the orientation of fibers.

Anisotropic swelling studies were carried out with rectangular samples cut at different angles with respect to orientation of the fiber from the tensile sheets and swollen in toluene at room temperature for 3 days. The length, breadth, and thickness of the samples were measured before and after swelling.

Scanning electron microscopy (SEM) studies were conducted with a Jeol JSM 5800 to analyze the fracture behavior of the composites. The fracture ends of the tensile and tear specimens were mounted on aluminum stubs and gold-coated to avoid electrical charging during examination.

TABLE II
Formulation of the Mixes

Ingredient	Gum	B	C	D	E	F	G	A	H	F′	G′	H′
NR	100	100	100	100	100	100	100	100	100	100	100	100
ZnO	5	5	5	5	5	5	5	5	5	5	5	5
Stearic acid	1.5	1.5	1.5	1.5	1.5	1.5	1.5	1.5	1.5	1.5	1.5	1.5
TDQ	1	1	1	1	1	1	1	1	1	1	1	1
CBS	0.6	0.6	0.6	0.6	0.6	0.6	0.6	0.6	0.6	0.6	0.6	0.6
Sulfur	2.5	2.5	2.5	2.5	2.5	2.5	2.5	2.5	2.5	2.5	2.5	2.5
Sisal fiber		5	10	20	25	21	21	21	21	21	21	21
Fiber length (mm)		10	10	10	10	2	6	10	15	10	10	10
Oil palm fiber		5	10	20	25	9	9	9	9	9	9	9
Fiber length (mm)		6	6	6	6	6	6	6	6	2	10	15

TABLE III
Fiber Length Distribution Index

	Sisal		Oil palm	
	Before mixing	After mixing	Before mixing	After mixing
L_n	10.28	9.89	11	10.8
L_w	8.688	8.4	10.2	9.8
L_w/L_n	0.845	0.849	0.927	0.9074

RESULTS AND DISCUSSION

Evaluation of fiber breakage

We estimated the extent of fiber breakage during mixing by immersing 1 g of the unvulcanized mix containing individual sisal and oil palm fibers in toluene to dissolve the rubber component and thus separate the fibers intact. One hundred counts were made to determine the fiber length distribution. The fibers were washed with toluene to ensure complete removal of rubber from the surfaces. The washed fibers were then collected and examined under a traveling microscope.

The control of the fiber length and aspect ratio of the fibers in a rubber matrix is difficult because of fiber breakage during processing. The severity of fiber breakage depends mainly on the type of fiber, the initial aspect ratio, and the magnitude of stress and strain experienced by the fibers during processing.[15,16]

The breakage of fibers due to high shear forces caused during mixing can be indicated by a fiber length distribution curve. The distribution of fiber lengths can be represented in terms of moments of the distribution. The number- and weight-average fiber lengths can be defined as:

$$L_n = \frac{\sum N_i L_i}{\sum N_i} \quad (1)$$

$$L_w = \frac{\sum N_i L_i^2}{\sum N_i L_i} \quad (2)$$

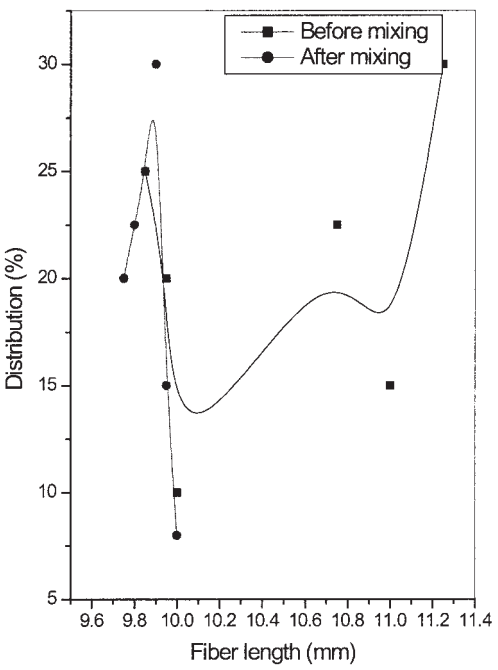

Figure 1 Fiber length distribution curve of the composites containing sisal fiber.

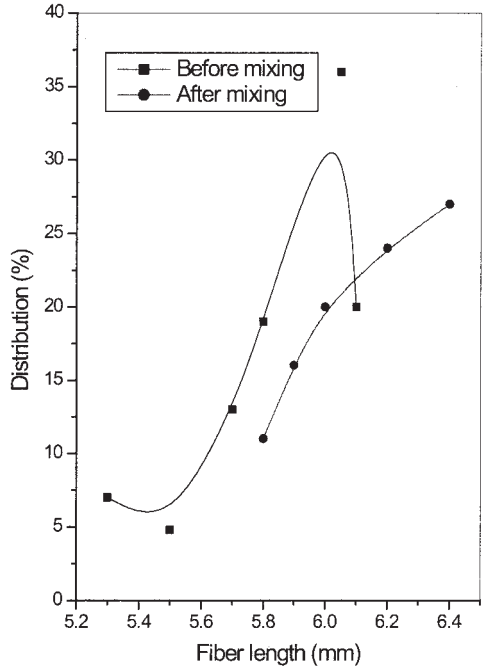

Figure 2 Fiber length distribution curve of the composites containing oil palm fiber.

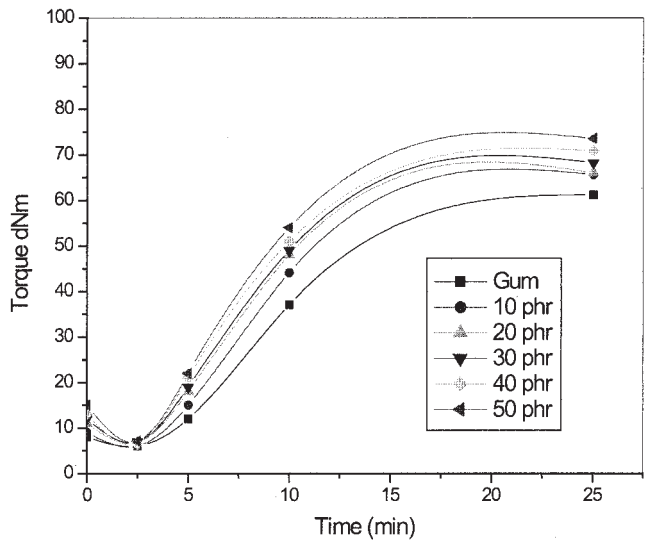

Figure 3 Torque–time curve at different fiber loadings.

TABLE IV
Cure Characteristics of the Various Mixes

Mix	T_{max} (dNm)	T_{min} (dNm)	ΔT	t_{90}
Gum	58	6	52	14
B	64	6	58	7.3
C	65.5	6.8	58.7	7.2
A	66	7	59	7
D	68	6.5	61.5	7.5
E	69	7.1	61.9	7.5

where L_n is the number-average fiber length, L_w is the weight-average fiber length, and N_i the number of fibers with length L_i. The value of L_w/L_n, the polydispersity index, can be taken as a measure of the fiber length distribution. The values of L_n, L_w, and L_w/L_n were calculated based on 50 fibers for the chopped sisal and oil palm fibers extracted from the mix. The fiber length distribution indices of the untreated sisal and oil palm fibers before and after mixing are given in Table III. The value of L_w/L_n remained about the same before and after processing, indicating that there was not considerable fiber breakage.

The fiber length distribution curves of the composites containing untreated sisal and oil palm fibers with lengths of 10 and 6 mm, respectively, are given in Figures 1 and 2. Figure 1 shows the fiber length distribution curve of untreated sisal fibers before and after mixing. After mixing, the majority of fibers were distributed between 9.7 and 10 mm. Figure 2 depicts the fiber length distribution curve of untreated oil palm fibers of with lengths of 6 mm before and after mixing. Here, the majority of fibers had lengths between 5.8 and 6 mm after mixing. The breaking of both sisal and oil palm fibers were low. As both fibers are lignocellulosic, they undergo bending and curling rather than breaking during milling. The average diameter of the sisal fibers (0.11 mm) and oil palm fibers (0.15 mm) remained the same after mixing.

Processing characteristics

The processability of the compounds were studied from the rheographs. The minimum torque in the rheograph gave an indication of the filler content in the rubber, whereas the maximum torque in the rheograph was a measure of the crosslink density and stiffness in the rubber. In general, for all of the mixes, the torque initially decreased, then increased, and finally leveled off. The initial decrease in torque to a minimum value was due to the softening of the rubber matrix, whereas the increase in torque was due to the crosslinking of the rubber. The leveling off was an indication of the completion of curing. Generally, the presence of fibers increased the maximum torque.

Effect of fiber loading

Figure 3 shows the rheographs of mixes G, B, C, A, D, and E. The presence of fibers generated an increase in the viscosity of the mixes. The increment in torque values with increasing fiber loadings indicated that as more and more fiber got into the rubber matrix, the mobility of the macromolecular chains of the rubber decreased, which resulted in more rigid vulcanizates.[17] Table IV shows the maximum torque, minimum torque, and cure time values for various mixes. The cure time was independent of the fiber loading.

Mechanical properties

Effect of fiber length

The properties of short fiber-reinforced elastomer composites depend on the degree to which an applied load is transmitted to the fibers. The extent of load transmittance is a function of the fiber length and the magnitude of the fiber–matrix interaction. At a critical fiber length (l_c), the load transmittance from the matrix to the fiber is at a maximum. If l_c was greater than the length of the fiber, the stressed fiber debonds from the matrix and the composite fails at a low load.

Table V shows the effect of fiber length on the tensile strength, elongation at break, and tensile modulus at 100% elongation. All of these properties were at a maximum when the lengths of the sisal and oil palm fibers were 10 and 6 mm, respectively. At higher

TABLE V
Effect of the Fiber Length on the Mechanical Properties of the Mixes

	Orientation	Gum	F (2.6 mm)	G (6.6 mm)	A (10.6 mm)	H (15.6 mm)	F′ (10.2 mm)	G′ (10.10 mm)	H′ (10.15 mm)
Modulus at 100% elongation	L	0.759	1.665	1.494	2.228	2.558	2.198	2.064	1.589
	T	0.895	1.54	2.052	1.251	2.233	2.153	2.001	1.577
Tensile strength (MPa)	L	14.4	4	4.512	8.3	6.01	7.8	5.5	3.9
	T	14.2	3.9	3.91	5.7	3.917	7.1	5.2	3.8
Tear strength (kN/m)	L	19	24.7	26.8	37.34	29.48	34	25	22
	T	17.9	21.57	30.2	35.38	37.34	35.6	23	20
Elongation at break (%)	L	890	519	668	794	513.6	799	630	526
	T	881	510	661	738	398	740	628	520

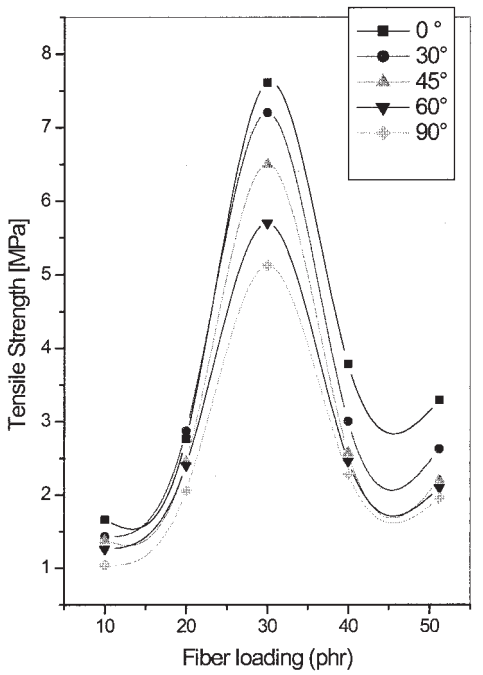

Figure 4 Variation of tensile strength with fiber loading.

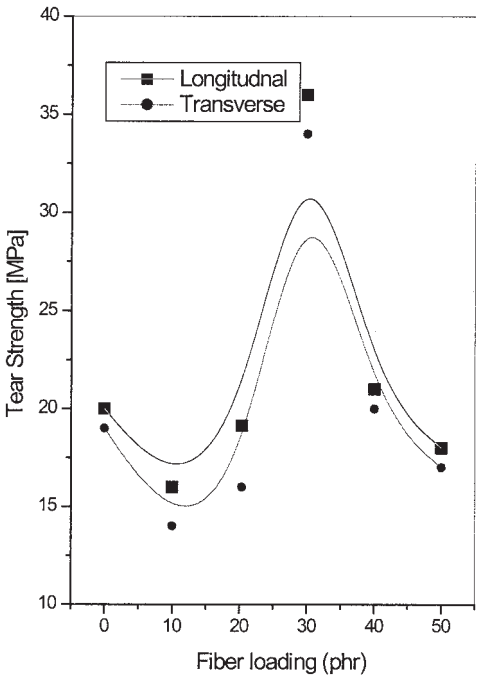

Figure 6 Variation of tear strength with fiber loading.

fiber lengths, a decrease in the properties were found. This was due to fiber entanglements prevalent at longer fiber lengths. From the overall mechanical property studies, we found that optimum fiber lengths of 10 and 6 mm for sisal and oil palm fibers, respectively, were effective for reinforcement in the NR matrix.

Effect of fiber loading

The effect of fiber loading on the tensile strength in short-fiber-reinforced NR composites has been widely studied.[18–20] Generally, the tensile strength initially drops up to a certain amount of fiber and then increases.

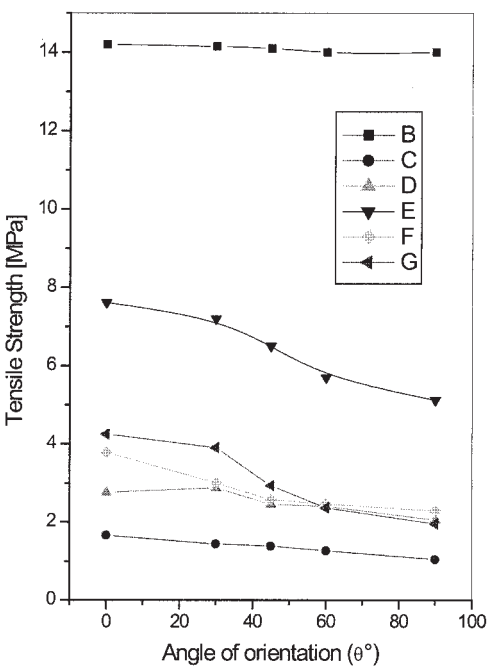

Figure 5 Variation of tensile strength with angle of orientation at different levels of fiber loading.

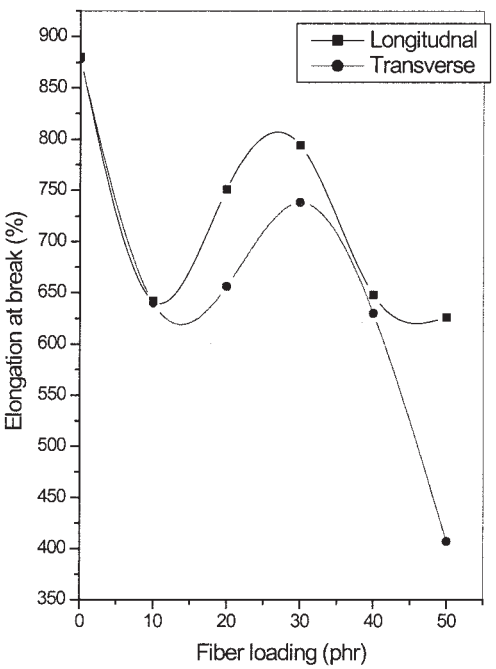

Figure 7 Variation of elongation at break with fiber loading.

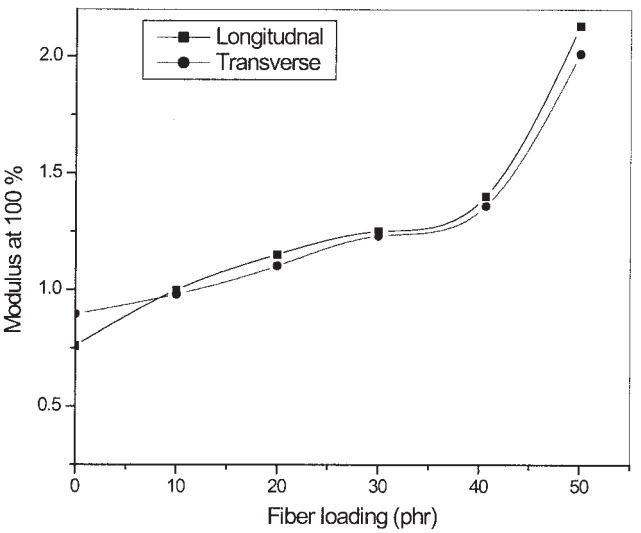

Figure 8 Variation of modulus at 100% elongation with fiber loading.

In this study, the behavior of the composites containing 10, 20, 30, 40, and 50 phr untreated sisal and oil palm fibers were analyzed. Sisal and oil palm fibers were taken in the ratio 50:50. As is clear in Figure 4, the tensile strength increased up to 30 phr and then declined. The tensile strength in the transverse direction also showed the same trend.

NR inherently possesses a high strength because of strain-induced crystallization. When fibers are incorporated into NR, the regular arrangement of rubber molecules is disrupted, and hence, the ability for crystallization is lost. This is the reason fiber-reinforced NR composites possess lower tensile strengths than gum compounds.

When fiber-reinforced rubber composites are subjected to load, the fibers act as carriers of the load, and stress is transferred from the matrix along the fibers, which leads to effective and uniform stress distribution, which results in good mechanical properties for the composite. The uniform distribution of stress is dependent on two factors: (1) the population and (2) the orientation of the fibers.

TABLE VI
Green Strength Values and Orientation

Mix (phr)	S_L (MPa)	S_T (MPa)	Orientation (%)
Gum	0.34	0.31	—
10	0.4	0.39	48
20	0.5	0.2	69.6
30	0.61	0.18	75.5
40	0.58	0.19	73.9
50	0.49	0.21	67.6

At low levels of fiber loading, the orientation of the fibers is poor, and the fibers are not capable of transferring load to one another, and stress gets accumulated at certain points in the composite, which leads to a low tensile strength. At high levels of fiber loading, the increased population of fibers leads to agglomeration, and stress transfer gets blocked. At intermediate levels of loading (30 phr), the population of the fibers is just right for maximum orientation, and the fibers actively participate in stress transfer.

The variation of composite tensile strength with the angle of orientation at different levels of fiber loading is given in Figure 5. The longitudinal orientation of fibers resulted in a maximum tensile strength, and as the angle of orientation of the fibers increased, the tensile strength decreased. When the fibers were longitudinally oriented, the fibers were aligned in the direction of force, and the fibers transferred stress uniformly. When transversely oriented, the fibers were aligned perpendicular to the direction of load, and they could take part in stress transfer.

Figure 6 shows the variation of tear strength with fiber loading. As loading increased, the tear strength at first decreased and, at 30 phr, showed an increase. At high fiber loadings, the tear strength decreased

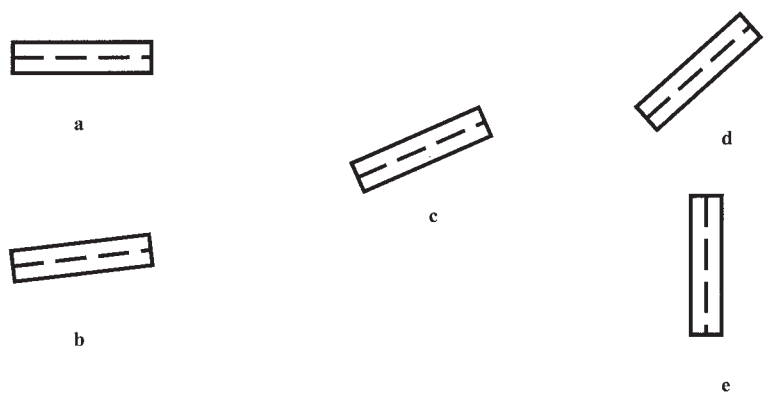

Figure 9 Schematic sketch of samples cut at different angles with respect to fiber orientation: (a) 0, (b) 30, (c) 45, (d) 60, and (e) 90°.

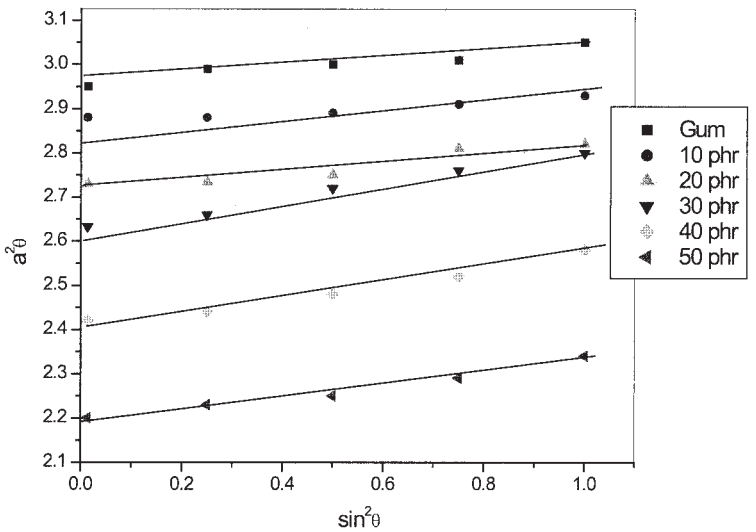

Figure 10 Swelling variation as a function of θ.

as the increased strain in the matrix between closely packed fibers increased tearing and reduced the tear strength. Similar results were observed by Ismail et al.[21]

Figure 7 presents the variation of elongation at break with fiber loading. The value of elongation at break showed a reduction with increasing fiber loading. Increased fiber loading in the rubber matrix resulted in composites becoming stiffer and harder. This reduced the composites' resilience and toughness and led to lower resistance to break.

The variation of modulus at 100% elongation with fiber loading is given in Figure 8. The values showed a steady increase with fiber loading.

Extent of fiber orientation from green strength measurements

The green strength of short-fiber-reinforced composites depends on the degree of fiber orientation, and so the latter can be obtained from the expression

$$\% \text{ Fiber orientation} = \frac{S_L/S_{G,L}}{S_L/S_{G,L} + S_T/S_{G,T}} \qquad (3)$$

where S is the green strength and the subscripts G, L, and T represent gum, longitudinal, and transverse, respectively. The effect of fiber loading on percentage orientation is given in Table VI. The percentage orientation was the lowest when the fiber loading was small, that is, 10 phr. At low fiber loadings, the fibers could randomly move around, which led to increased chaoticity and decreased levels of orientation. As the fiber loading increased, the percentage orientation increased with the maximum value for the composite containing 30 phr fibers. At a 40-phr fiber loading, the percentage orientation decreased, indicating that the fibers could not orient themselves because of entanglement caused by the increased population of fibers.

Anisotropic swelling studies

Anisotropic swelling studies were carried out with rectangular samples cut at different angles with respect to the orientation of the fiber from the tensile sheets. This is schematically represented in Figure 9. For short-fiber-reinforced rubber composites, the swelling ratio in any direction forming an angle (θ) with the fiber orientation is given by the expression

$$a_\theta^2 = (a_T^2 - a_L^2)\sin^2\theta + a_L^2 \qquad (4)$$

where a_L and a_T are the dimensional swelling ratios in the longitudinal and transverse directions, respectively. Figure 10 shows the dimensional swelling variation with θ in accordance with eq. (4) where various values of θ were assumed. For all of the mixes, the swelling increased with θ and was at a maximum when θ was 90°C. The line corresponding to the gum compound, which did not contain fibers, was posi-

TABLE VII
Slope Values from the Anisotropic Swelling Studies

Mix	Slope value
Gum	0.1427
B	0.153
C	0.153
A	0.1983
D	0.1673
E	0.1522

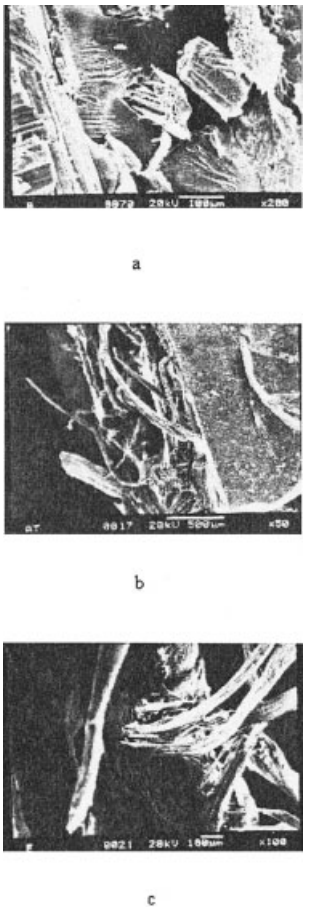

Figure 11 Scanning electron micrographs of the tensile fracture specimens: (a) 10, (b) 30, and (c) 50 phr.

tioned above those for the other mixes. This showed that short fibers restricted the transport of solvent into the composite.

The extent of fiber alignment can be understood from the slope values given in Table VII. It was reported[22] that the steeper the line is, the higher the degree of fiber alignment is. Mix A showed the maximum slope value among the various mixes. This showed that the composite containing 30 phr fiber had the highest degree of fiber alignment.

SEM studies have been used extensively to study fiber/matrix interaction. SEM observations indicated that there was a certain difference in the fiber/matrix interaction, depending on the loading of the composites. Figure 11(a–c) shows the scanning electron micrographs of the fractured tensile specimens of the composites containing 10, 30, and 50 phr fiber. As shown in Figure 11(a), there was a fiber pullout, indicating not much fiber/matrix interaction as there were only a few fibers, and they could not participate in stress transfer. At high fiber loadings [Fig. 11(c)], there was an agglomeration of fibers, which led to the formation of bundles. These bundles acted as barriers to stress transfer, and hence, the interface was weak. As shown in Figure 11(b), there was fiber breakage because of the strong fiber/matrix adhesion as the population of fibers was just right for effective stress transfer.

CONCLUSIONS

The processability characteristics and mechanical properties of NR composites reinforced by sisal/oil palm hybrid fibers were investigated as a function of fiber length and loading. Fiber breakage analysis revealed that the extent of breaking of the sisal and oil palm fibers was low. The mechanical properties of the composites in the longitudinal direction were superior to those in the transverse direction. The optimum lengths for the sisal and oil palm fibers were 10 and 6 mm, respectively. The addition of sisal and oil palm fibers led to a decrease in the tensile strength and tear strength but an increase in the modulus. Cure time was found to be independent of fiber loading. Anisotropic swelling studies indicated that the presence of short fibers restricted the entry of solvent. SEM studies revealed that fiber/matrix interaction was poor at low and very high fiber loadings.

References

1. Goettler, L. A.; Shen, K. S. Rubber Chem Technol 1983, 620, 56.
2. Setua, D. K.; De, S. K. J Mater Sci 1984, 8, 18.
3. Oksman, K.; Clemons, C. J Appl Polym Sci 1998, 1503, 67.
4. Raj, R. G.; Kokta, B. V.; Maldas, D.; Daneault, C. J Appl Polym Sci 1989, 1089, 37.
5. Park, B. D.; Balatinecz, J. J Polym Compos 1997, 79, 18.
6. Sandi, A. R.; Rowell, R. M.; Caulfield, D. F. Polym News 1996, 7, 20.
7. Raj, R. G.; Kokta, B. V.; Maldas, D.; Daneault, C. J. Appl Polym Sci 1991, 1358, 31.
8. Yam, K. L.; Gogoi, B. K.; Lai, C. C.; Selke, S. E. Polym Eng Sci 1990, 693, 30.
9. Varghese, S.; Kuriakose, B.; Thomas, S.; Koshy, T. A. Indian J Nat Rubber Res 1991, 4, 55.
10. Geethamma, V. G.; Joseph, R.; Thomas, S. J Appl Polym Sci 1995, 55, 583.
11. Setua, D. K.; De, S. K. Rubber Chem Technol 1983, 808, 56.
12. Arumugam, N.; Tamareselvy, K.; Venkata Rao, K.; Rajalingam, P. J Appl Polym Sci 1989, 2645, 37.
13. Iannace, S.; Ali, R.; Nicolais, L. J Appl Polym Sci 2001, 79, 1084.
14. Sreekala, M. S.; Thomas, S.; Neelakantan, N. R. J Polym Eng 1997, 265, 16.
15. De, S. K.; Murty, V. M. Polym Eng Rev London 1984, 313, 4.
16. Pramanik, P. K.; Khastgir, D. K.; Saha, T. N. Plast Rubber Compos Proc Appl 1991, 15, 189.
17. Chakraborty, S. K.; Setua, D. K.; De, S. K. Rubber Chem Technol 1982, 1286, 55.
18. Geethamma, V. G.; Thomas Mathew, K.; Lakshminarayanan, R.; Thomas, S. Polymer 1998, 39, 1483.
19. Prasantha Kumar, R.; Geethakumari Amma, M. L.; Thomas, S. J Appl Polym Sci 1995, 597, 58.
20. Varghese, S.; Kuriakose, B.; Thomas, S. Plast Rubber Comp Proc Appl 1993, 930, 20.
21. Ismail, H.; Rosnah, N.; Rozman, H. D. Polymer 1997, 16, 38.
22. Noguchi, T.; Ashida, M.; Mashimo, S. Nippon Gomu Kyokaishi 1984, 171, 57.